Supporting Information

Cheng et al. 10.1073/pnas.1207354109

SI Materials and Methods

Generation of *Stim1–Stim2* Double-KO Mice and Assessment of Saliva Secretion. T-cell–specific deletion of *Stim1* and *Stim2* and generation of the double-KO (DKO) mice were done as described previously (1). In the experiments described here, the litter-matched mice [control (CTRL) and *Stim1–Stim2* DKO] were used between 3 wk and 12 wk of age. Only female mice were used in the study. Mice were anesthetized with ketamine (60 mg/kg i.m.) and xylazine (8 mg/kg i.m.), and saliva was collected after treatment with pilocarpine (0.5 mg/kg s.c.). All mice were maintained in specific pathogen-free barrier facilities at Harvard Medical School and were used in accordance with protocols approved by the Center for Animal Resources and Comparative Medicine of Harvard Medical School and conformed to relevant guidelines and laws.

Determination of Autoantibodies. Serum samples of 12-wk-old DKO mice and CTRL mice were analyzed for autoantibodies against Sjögren's syndrome A SSA/Ro and Sjögren's syndrome B SSB/La using a commercially available ELISA kit (Alpha Diagnostic International) in accordance with the manufacturer's protocol. Plates were analyzed with a microplate reader reading at 490 nm.

Morphological Assessment of Salivary Glands. For histochemistry, salivary glands were embedded in paraffin, then sectioned (5 μm each) and stained with H&E. The focus score (FS) was defined as an aggregate of 50 or more lymphocytes per 4 mm^2 of salivary gland tissue. For immunofluorescence, excised salivary glands were fixed in 10% (vol/vol) formalin and embedded in paraffin. Then 5-μm sections of tissue were blocked with 20% donkey serum (Jackson ImmunoResearch) and treated with the required primary antibody—rabbit polyclonal anti-human aquaporin-5 (AQP5; Alomone Labs), rabbit polyclonal anti-human CD3 (Dako), rabbit polyclonal anti-human STIM1 (Cell Signaling), or rabbit polyclonal anti-cow wide-spectrum cytokeratin (Dako)—and required secondary antibodies. Samples were mounted with Vectashield antifade reagent with DAPI (Vector Laboratories) and imaged with a Leica LSM-SP2 confocal microscope.

Acquisition of Peripheral Blood Mononuclear Cells from Patients with Primary Sjögren's Syndrome. Samples were obtained from 27 patients with primary Sjögren's Syndrome (pSS; all females) and 17 CTRL subjects (15 females and 2 males, in which 8 were assigned a low FS but diagnosed as healthy) enrolled in Sjögren's syndrome studies at the National Institute of Dental and Craniofacial Research and the National Institute of Arthritis and Musculoskeletal and Skin Diseases. Informed consent was obtained from all patients and controls. All studies were approved by the Institutional Review Boards of National Institute of Dental and Craniofacial Research and Nationasl Institute of Diabetes and Digestive and Kidney Disorders/National Institute of Arthritis and Musculoskeletal and Skin Diseases. All CTRL subjects and pSS patients underwent a standardized evaluation for Sjögren's syndrome that included oral and ophthalmologic examinations, laboratory testing, and a rheumatologic evaluation or a chart review by a rheumatologist at the National Institutes of Health. Minor salivary gland (MSG) biopsy specimens were obtained from six patients and four healthy controls. Peripheral blood mononuclear cells (PBMCs) were obtained from blood samples using BD Vacutainer CPT tubes.

Western Blot Analysis. PBMC samples were lysed in RIPA buffer supplemented with Complete Protease Inhibitor Mixture tablets (Roche Diagnostics). Lysates were centrifuged at 12,000 × *g*. Then the supernatants were mixed with NuPAGE LDS Sample Buffer (Invitrogen) and resolved on SDS/PAGE gels, which were used for Western blots using rabbit polyclonal anti-human STIM1 or STIM2 (Cell Signaling), rabbit polyclonal anti-human GAPDH (Abcam), or rabbit polyclonal anti-human CD3 (Dako) for detection.

$[Ca^{2+}]_i$ Imaging. For $[Ca^{2+}]_i$ measurements in Fura-2–loaded PBMCs, the cells were first allowed to attach to poly-L-lysine–coated glass-bottomed tissue culture dishes (MatTek) for 15 min. Measurements were made in perfused cells stimulated with 1 μM thapsigargin or 10 μg/mL of anti-CD3 antibody (OKT3; eBioscience) for 10 min at 22–25 °C. Fura-2 fluorescence was measured using a Till Photonics-Polychrome V spectrofluorimeter with MetaFluor imaging software (Molecular Devices). Each fluorescence trace (340/380 ratio) represents an average of at least 50–150 individual cells from more than four individual experiments.

Statistics. Data analysis was performed using Origin 8 (OriginLab). Statistical comparisons were made using the Student *t* test. Experimental values are expressed as mean ± SD or mean ± SEM. Differences in the mean values were considered significant at $P < 0.05$.

1. Oh-Hora M, et al. (2008) Dual functions for the endoplasmic reticulum calcium sensors STIM1 and STIM2 in T cell activation and tolerance. *Nat Immunol* 9:432–443.

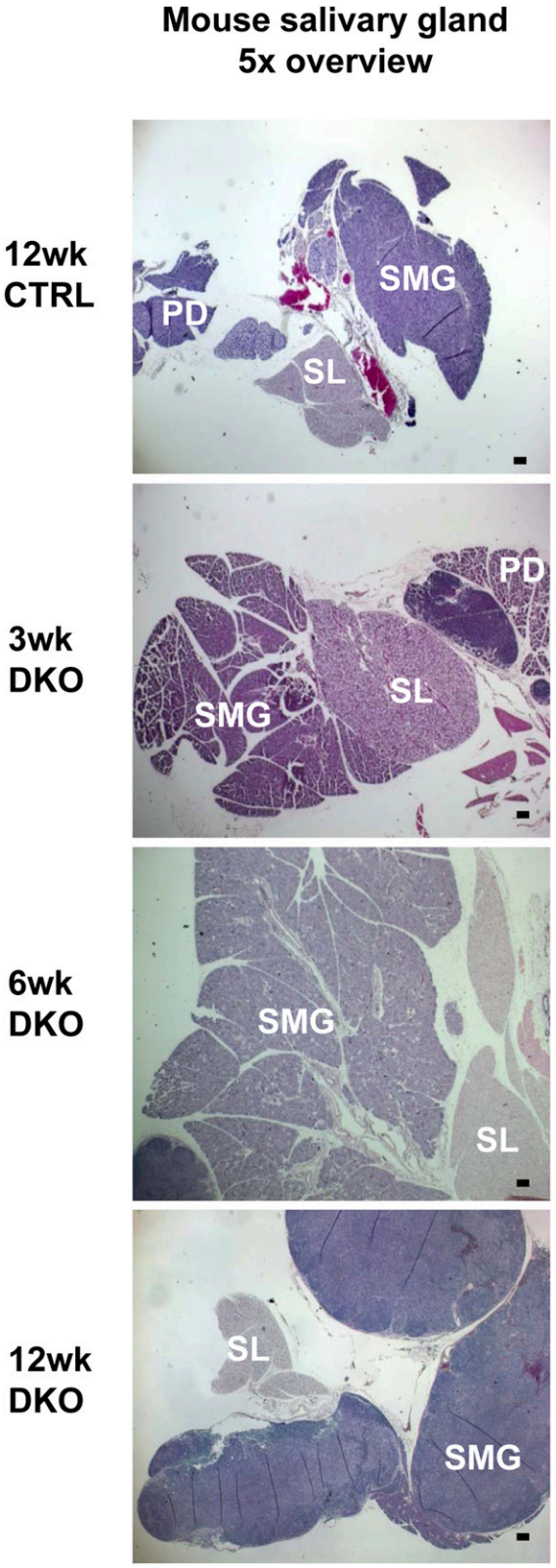

Fig. S1. Morphological analysis of submandibular glands from CTRL and DKO mice. H&E staining of salivary glands from 3-, 6-, and 12-wk-old CTRL and DKO mice. Different glands can be seen in the field (SMG, submandibular; SL, sublingual; PD, parotid). DKO mice exhibit a progressive decrease in healthy submandibular gland tissue and an increase in infiltration, which becomes very large and diffuse in the 12-wk-old animals. (Original magnification 10×; scale bar: 100 μm.)

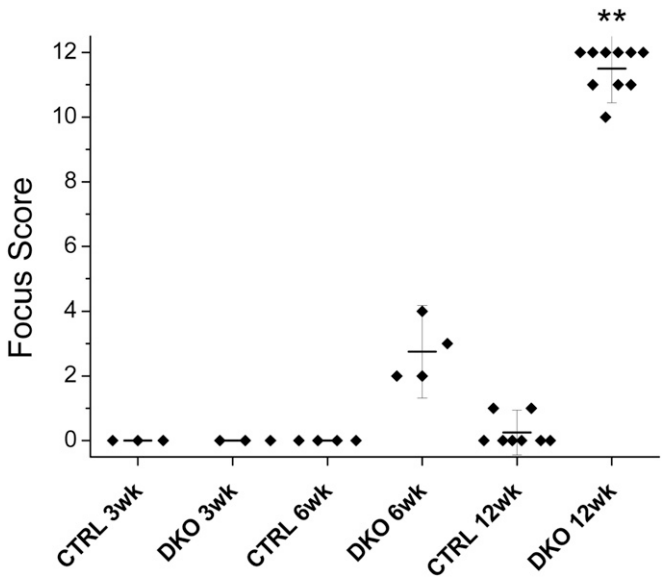

Fig. S2. FS analysis in CTRL and DKO mice. Salivary glands were removed for histological analysis at 3 wk, 6 wk, and 12 wk, then fixed and stained with H&E. Histopathological assessment data are presented as FS (6-wk-old DKO, 2.75 ± 0.96; 12-wk-old DKO, 11.5 ± 0.71). Data are mean ± SD. $^{**}P < 0.01$.

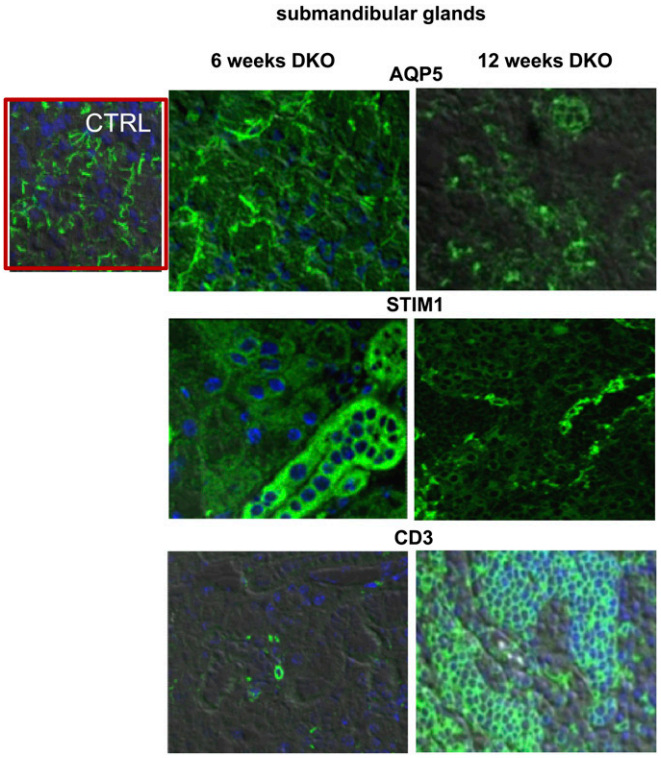

Fig. S3. Progressive disruption of AQP5 and STIM1 and $CD3^+$ cell infiltration in submandibular glands from DKO mice. Enlarged areas of images shown in Fig. 4. Immunolocalization of AQP5, STIM1, and CD3 in 6-wk-old and 12-wk-old DKO mouse submandibular gland. (*Inset*) CTRL mouse gland, with AQP5 and CD3 images are overlaid over the DIC image of the field. A progressive loss of AQP5 and STIM1 within the gland and an increase in $CD3^+$ infiltrating cells are shown.

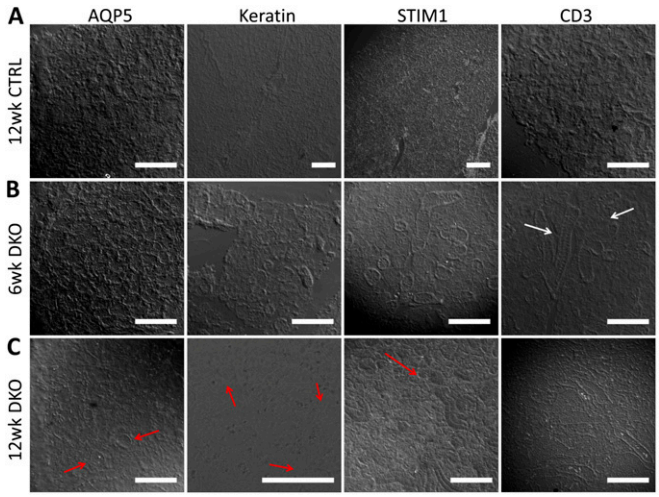

Fig. S4. Expression of salivary gland marker proteins in submandibular glands from CTRL and DKO mice. DIC images of the areas shown in Fig. 4.

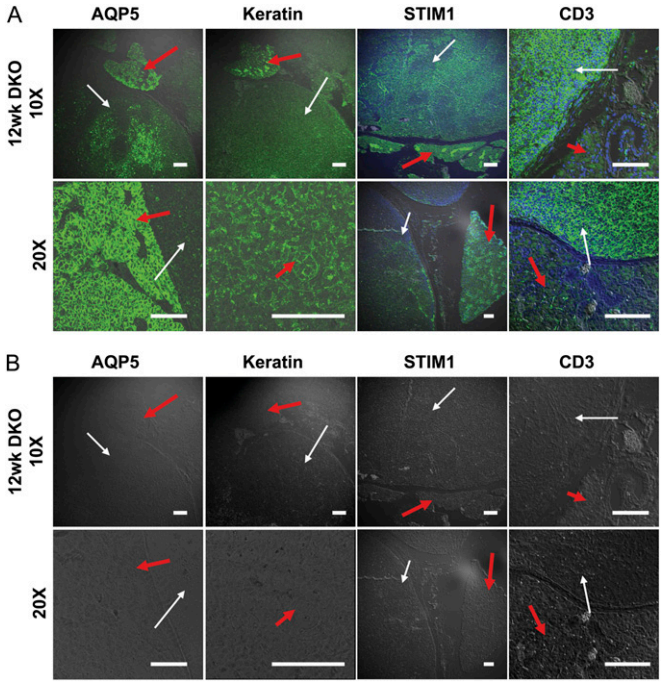

Fig. S5. Localization of salivary gland marker proteins, STIM1, and CD3$^+$ cells in samples of submandibular glands from 12-wk-old DKO mice. (*A*) Localization of AQP5 (acinar cell marker), keratin (epithelial cell marker), STIM1, and CD3 in submandibular gland secretions from 12-wk-old DKO mice. Images were acquired at 10× and 20× magnification and are overlaid with DIC. (*B*) Separated DIC images showing the structure of salivary gland tissue. (Scale bars: 100 μm.) Labeling and other details are described in the text. White arrows indicate inflamed areas of the gland; red arrows, residual healthy tissue.

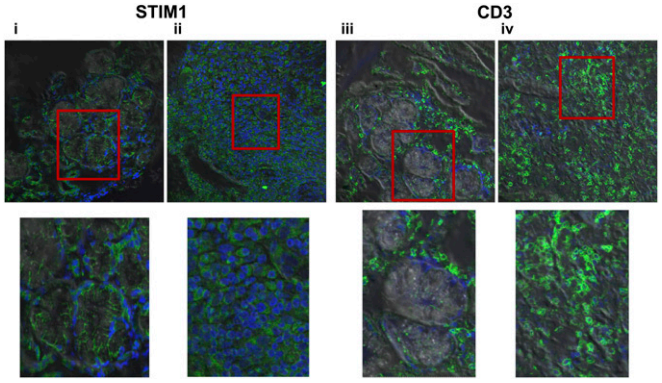

Fig. S6. Pattern and expression of STIM1 in MSG tissue biopsy specimens from pSS patients with severe lymphocytic infiltration. MSG biopsy samples from high-FS pSS were assessed for STIM1 and CD3 expression. Images are enlarged images of the high-FS samples shown in Fig. 5. The area indicated by the red box was enlarged to show STIM1 and $CD3^+$ cells in residual healthy region of the gland (*i* and *iii*), as well as in disrupted infiltrated area of the gland (*ii* and *iv*). All images are overlaid on the DIC image of the field. Acinar and ductal structures are visible in *i* and *iii*, but not in *ii* and *iv*. In *ii*, the area of intense blue indicates nuclei of infiltrating mononucleocytes. This region showed relatively poor STIM1 staining. In contrast, areas containing relatively high $DAPI^+$ nuclei stained strongly for CD3.

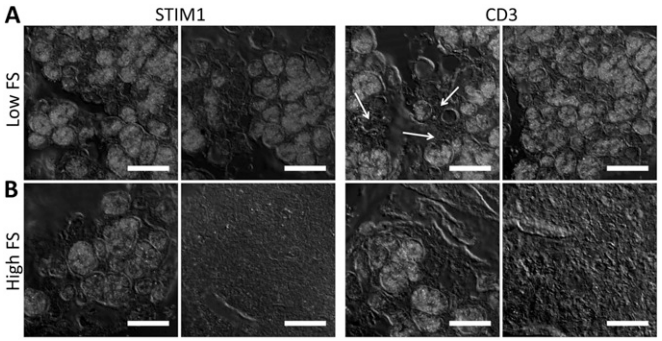

Fig. S7. DIC images of immunofluorescence displayed in Fig. 5 in MSG biopsy specimens from low-FS (*A*) and high-FS (*B*) pSS patients. (Scale bars: 100 μm.)

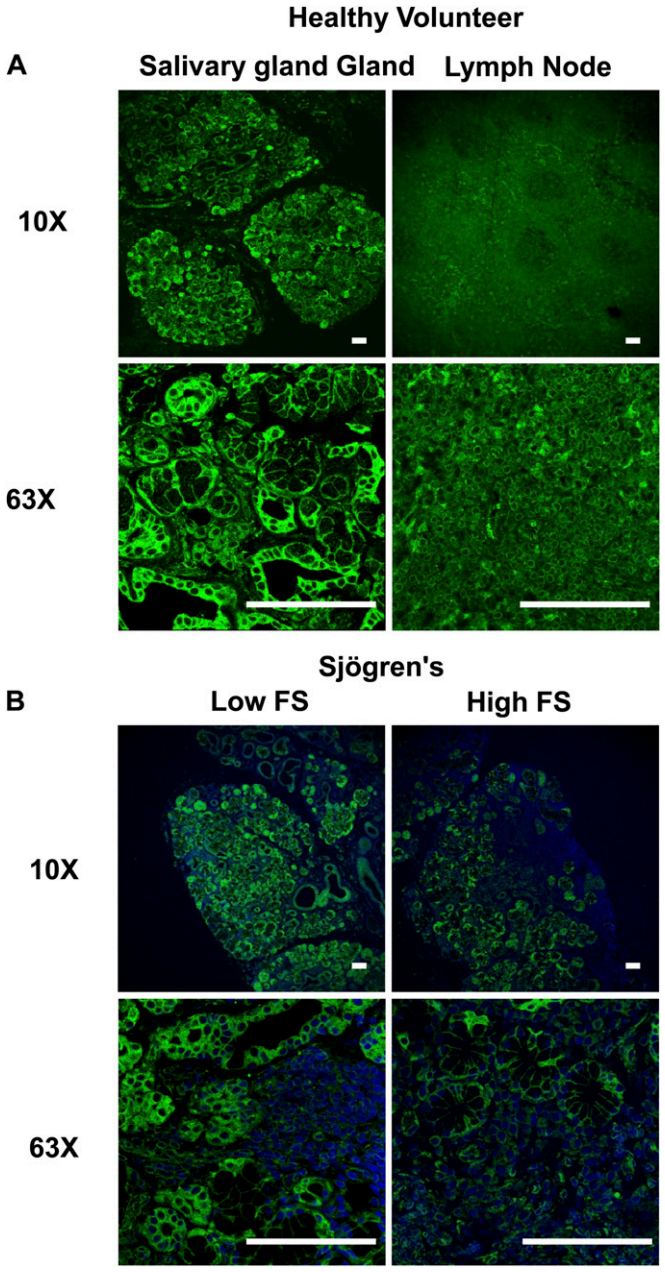

Fig. S8. STIM1 localization in MSG and cervical lymph node specimens from healthy volunteers. (*A*) STIM1 was examined in MSG and cervical lymph node specimens from healthy individuals. Both 10× and 63× images are shown. STIM1 labeled all areas of the MSG and lymph node. (*B*) STIM1 localization in MSG biopsy specimens from low-FS and high-FS patients. Disruption of STIM1 in high-FS patients was confirmed in a second patient (see also the data in Fig. 5 and Fig. S6). Decreased amounts of STIM1 in glands from high-FS patients as well as in STIM1 in infiltrating areas can be seen. (Scale bars: 100 μm.)